Decay and damage of therapeutic phage OMKO1 by environmental stressors

Michael Blazanin[1,⊗,*], Wai Tin Lam[1,⊗], Emma Vasen[1], Benjamin K. Chan[1], and Paul E. Turner[1,2]

[1]Department of Ecology and Evolutionary Biology, Yale University, New Haven, CT 06511, USA.

[2]Program in Microbiology, Yale School of Medicine, New Haven, CT 06520, USA.

[⊗]These authors contributed equally to the work, and are listed in alphabetical order.

*Correspondence to: Mike Blazanin, Department of Ecology and Evolutionary Biology, Yale University, 165 Prospect St, New Haven, CT, 06520, USA; mike.blazanin@yale.edu

Keywords: bacteriophage, thermotolerance, virus

Short title: Tolerance of OMKO1 to environmental stress

Abstract

Antibiotic resistant bacterial pathogens are increasingly prevalent, driving the need for alternative approaches to chemical antibiotics when treating infections. One such approach is bacteriophage therapy: the use of bacteria-specific viruses that lyse (kill) their host cells. Just as the effect of environmental conditions (e.g. elevated temperature) on antibiotic efficacy is well-studied, the effect of environmental stressors on the potency of phage therapy candidates demands examination. Therapeutic phage OMKO1 infects and kills the opportunistic human pathogen *Pseudomonas aeruginosa*. Here, we used phage OMKO1 as a model to test how different environments affect the decay rate of a therapeutic virus, and whether exposure to an environmental stressor can damage surviving viral particles. We assessed the effects of elevated temperatures, saline concentrations, and urea concentrations. We observed that OMKO1 particles were highly tolerant to different saline concentrations, but decayed more rapidly at elevated temperatures and under high concentrations of urea. Additionally, we found that exposure to elevated temperature reduced the ability of surviving phage particles to suppress the growth of *P. aeruginosa*, suggesting a temperature-induced damage. Our findings demonstrate that OMKO1 is highly tolerant to a range of conditions that could be experienced inside and outside the human body, while also showing the need for careful characterization of therapeutic phages to ensure that environmental exposure does not compromise their expected potency, dosing, and pharmacokinetics.

Introduction

Widespread use of antibiotics – particularly in human therapy and animal agriculture – has selected for the evolution of multi-drug resistant bacterial pathogens, commonly associated with poorer prognosis and higher morbidity in human infections [1, 2]. One alternative or complementary approach to treating bacterial infections with chemical antibiotics is bacteriophage therapy [3], where bacteria-specific viruses with lytic replication cycles are used to kill (lyse) target bacterial cells. With any therapeutic treatment, understanding the effect of environmental conditions on efficacy is paramount. The effects of conditions like high temperature on the stability and application of chemical antibiotics is classically shown [4-7]. In parallel, during development of phage therapy it is important to measure the effects of various environmental conditions on the stability and subsequent reproduction on host cells of candidate therapeutic phages. Here, we use a therapeutic phage for a common human pathogen as a model of phage stability under a range of environmental conditions.

The need for novel approaches to treat bacterial pathogens varies greatly between infections: some strains of bacterial pathogens remain treatable with conventional antibiotics, while others show resistance across multiple drug classes, sometimes to all currently-approved antibiotics [8]. One of these multi-drug resistant bacterial pathogens is *Pseudomonas aeruginosa*, which has been identified by the World Health Organization as a high-priority threat to human health [9]. *P. aeruginosa* is a widespread gram-negative opportunistic pathogen that is commonly found in both natural habitats (e.g., soil, fresh water) and artificial environments (e.g., sewage, households, hospitals, and contaminated medical equipment) [10-13]. For these reasons, *P. aeruginosa* is frequently encountered by humans and causes urinary-tract and respiratory infections in immunocompromised individuals, as well as fouling surgically-implanted materials and devices [14, 15] . Individuals with cystic fibrosis (CF), non-CF bronchiectasis, and chronic-obstructive pulmonary disease (COPD) are especially vulnerable to lung infections caused by *P. aeruginosa*. Treatment of *P. aeruginosa* with chemical antibiotics is often ineffective, both because the bacteria readily form biofilms that limit the penetrance of antibiotic molecules, and due to multi-drug efflux (Mex) systems: protein complexes that actively remove various types of antibiotics from the cell [16-18].

As an alternative or complementary approach to treating *P. aeruginosa*, phage therapy has many attractive advantages, such as the ability for the phage 'drug' to self-amplify within the infection site. However, phage therapy also has some disadvantages, most notably the rapid evolution of bacterial resistance to lytic phage infection [19]. We previously described a naturally-occurring phage that leverages this inevitability of phage-resistance evolution as a strength. The dsDNA phage OMKO1 (virus family Myoviridae) attacks *P. aeruginosa*, while affecting the ability for the target bacteria to maintain resistance to various antibiotics [20, 21]. When bacterial strains evolve resistance to phage OMKO1, the mutants can show drug re-sensitivity, suggesting compromised ability for mechanisms such as MexAB and MexXY efflux pumps to remove antibiotics from the cell. Thus, phage OMKO1 can be doubly effective – the virus kills phage-susceptible bacterial cells, and also can drive evolution of phage resistance-associated loss of antibiotic resistance. This 'evolutionary tradeoff' is a mechanistic example of how phages can synergistically interact with chemical antibiotics, to beneficially extend the usefulness of currently-approved drugs. For example, phage OMKO1 and ceftazidime were used successfully in

emergency treatment of a 76-year-old patient, to resolve a chronic multi-drug resistant *P. aeruginosa* mediastinal and aortic graft infection [22]. We are also currently testing phage OMKO1 in a clinical trial to resolve or reduce *P. aeruginosa* infections in the lungs of CF, non-CF bronchiectasis and COPD patients when administered via aerosol-delivery (nebulizer) treatment ("CYPHY", NCT04684641).

While phage OMKO1 already has been used successfully for patient treatment, its stability across environmental conditions remains uncharacterized. Phages for therapeutic use can be manufactured in large volumes then stored, and treatment can be administered through various routes, including intravenous, oral suspension, nebulizer, and direct injection to the site of infection. However, it is well-known that virus particles can degrade over time (i.e., become inactivated for cellular infection), and that the rate of degradation can depend on the degree of environmental stress, including elevated temperature, and exposure to high concentrations of salt and urea [23-31]. Because degradation alters the concentration of active virus particles, it can create inaccuracies for treatment dosing and administration. In addition, depending on the sensitivity of phage particles to conditions present in the human body, environmentally-induced degradation could also play a role in the pharmacokinetics during treatment. Moreover, environmental conditions could have effects beyond degradation, potentially altering the growth and infectivity of viral particles which are still intact. Thus, it is vital to test how exposure to environmental stressors affects both the titer and activity of phage-therapy candidates. Here, we use phage OMKO1 as a general model to test the adverse biological effects of three environmental stressors (salt, urea, and heat) – within and beyond the conditions experienced in the human body – on the stability and subsequent infectivity of a virus successfully used in phage therapy.

Materials and Methods

Strains

P. aeruginosa strain PAO1 was provided by B. Kazmierczak (Yale School of Medicine) and cultured on 1.5% agar plates and liquid media made from Lysogeny Broth (LB: 10 g/L tryptone, 10 g/L NaCl, 5 g/L yeast extract). Bacteria were incubated at 37°C, and overnight batch cultures were grown with shaking (100 rpm) in 10mL broth, by inoculating with a single randomly-chosen colony. Bacterial stocks were stored in 40% glycerol at -80°C.

Phage OMKO1 was originally isolated from an aquatic sample (Dodge Pond, East Lyme, CT) enriched on PAO1 [20]. High-titer stocks (lysates) of the phage were obtained by mixing 10µl of the original stock with 10ml of PAO1 culture in exponential phase. After 12 hours to allow phage population growth, the mixture was centrifuged and filtered (0.22µm) to remove bacteria to obtain a cell free lysate. Phage lysates were stored at 4°C. Eight biological replicate OMKO1 stocks (S3, S8, S11, S16, R3, CV1, EV1, EV2) used in some experiments were generated by adding 10µl of the original stock into 5 independent 10ml PAO1 cultures in exponential phase. For simplicity, these were labeled stocks A, B, C, D, E, F, G, and H respectively.

Measuring Bacterial and Phage Densities

The density of a bacterial suspension was estimated using measurements of optical density at 600nm (OD600), based on a pre-generated standard curve for conversions between OD600 and colony forming units (CFU) per mL in a bacterial culture.

Estimates of phage titers were obtained via classic plaque-assay methods [32]. Lysate samples were serially diluted in LB, and 100 µL of phage dilution were mixed with 100 µL overnight PAO1 culture and added to 4 mL 'soft' (0.75%) agar LB held at 50°C. After gentle vortexing, the mixture was immediately spread onto a 1.5% agar LB plate. When solidified, plates were inverted and incubated overnight at 37°C. Plates with countable plaques were used to calculate the number of plaque-forming-units (PFUs) per mL in the lysate.

Heat stress survival

To measure effects of heat on phage stability, we exposed samples of phage OMKO1 to temperatures ranging from 55°C to 80°C for 5, 30, 60, or 90 minutes (Fig 1A), or 70 °C for 5, 90, 180, 270, or 360 minutes (Fig 1B). For each temperature-duration treatment 100 µL of an OMKO1 phage stock (stock A-E; for Fig 1A, only Stock A) stored in LB media was split evenly into two replicate 250 µL Eppendorf tubes and placed in a pre-heated MyCycler PCR block (BioRad Laboratories, Inc., Hercules, CA) with an established temperature gradient (30-80°C, at 5°C intervals). Tubes were removed from the heat block after specified times, and immediately cooled on ice to halt the stressful condition. The two replicate tubes were mixed together, and then titered in triplicate to measure phage densities. Percent survival was calculated relative to the density measured in the 55°C treatment after 5 minutes (Fig 1A), or relative to the source stock density (Fig 1B). We then fit a generalized linear model and carried out an ANCOVA. For Fig 1A, the model was of $\log_{10}$(percent survival) as a function of temperature (as a factor) and the interaction between temperature and duration; for Fig 1B, of $\log_{10}$(percent survival) as a function of phage stock and the interaction of phage stock and duration. Values below the limit of detection were excluded from statistical analyses.

Measuring phage fitness by bacterial growth curves

To measure phage fitness post heat stress, phages were subjected to heat stress as described above then titered. These samples were then normalized by concentration to combine a defined number of post-stress PFUs with bacteria in a 200 µL volume of LB in replicate wells (n = 3 or 6) of a 96-well plate (Corning Inc., Corning, NY). For most populations, 200 PFUs were inoculated in each well. However, because of low phage survival rates at longer heat shock times, some wells received fewer PFUs (Fig S3). Across all wells, however, bacteria and phage were inoculated at a constant multiplicity of infection (MOI; ratio of phage particles to bacterial cells) of 10^{-5}. Plates were incubated >12 hours at 37°C and an automated spectrophotometer (INFINITE F500 microplate reader, TECAN Schweiz AG, Männedorf, Switzerland) was used to monitor changes in the bacterial density (OD600) every 5 minutes, as described above. Growth curves were smoothed and the first local maximum optical density of the bacterial population was used as a reverse proxy for the fitness of phage (Fig S2) [33, 34] (see R script at https://github.com/mikeblazanin/tin-omko1). We then fit a linear model and carried out an ANOVA for peak bacterial density as a function of heat shock treatment (as a factor), phage stock, and treatment-stock interaction. Treatments which were not initially inoculated with 200 PFUs were excluded from

statistical analyses. Post-hoc pairwise comparisons between all levels of the heat shock treatment were performed with Tukey's Honest Significant Differences.

Urea & salt stress survival

To measure the effects of urea (carbamide) and salt (NaCl) on phage stability, 10 µL of phage stock F, G, or H was added to 990 µL of either urea or salt solution at a defined concentration, and vortexed to mix thoroughly. For saline, these included 0M, 0.5M, 3M, 5M, and an LB control (0.17M). For urea, these included 0M, 1M, 2M, 3M, and 4M. One replicate of each of the three phage stocks was exposed to each concentration. At 45 and 90 minutes, subsamples were obtained by removing 50 µL and immediately diluting 200-fold to terminate the stress condition. Then, the stressed samples were titered in triplicate to calculate survival following stress, with percent survival calculated relative to the control titer (for saline, LB; for urea, 0M) at 0 minutes. We then fit a generalized linear model and carried out an ANCOVA of $\log_{10}$(percent survival) as a function of urea or saline concentration (as a factor) and the interaction between concentration and duration. Values below the limit of detection were excluded from statistical analyses.

Analysis

All analysis was carried out in R (3.6.0) using dplyr (0.8.2), figures were made using ggplot2 (3.2.0) and ggsignif (0.6.0) [35-38]. All data analysis and visualization code is available at https://github.com/mikeblazanin/tin-omko1

Results

To estimate the tolerance of phage OMKO1 to heat stress, we measured phage particle survival over time at different temperatures. Temperature shock significantly increased phage OMKO1 decay rate (Fig 1A, ANCOVA, $F(4, 8) = 125.01$, $p < 0.001$). At the two lowest temperatures (55°C and 60°C), there was no significant evidence of OMKO1 decay over time (Table 1). However, at 65°C there was a significant moderate signal of decay, which became more pronounced at 70°C. At 75°C and 80°C, phage particles decayed so rapidly that most measures in these environments were unobtainable (i.e., fell below the limit of detection). Abnormal plaque morphology was also observed in heat-treated phages (data not shown), suggesting possible phenotypic alteration of phage OMKO1 following heat treatment, explored further below.

Table 1. Multiple regression shows significant phage OMKO1 decay at 65°C and higher temperatures. Parameter estimates of the rate of decay over time (slope) depending on temperature were evaluated to detect increased decay (decreased slopes) against the null hypothesis of 0 slope using one-tailed t-tests (df = 8) and a Bonferroni correction (4 tests).

Temperature (°C)	Estimated Coefficient	t-value	Bonferroni-adjusted p-value
55	0.0008	0.98	1
60	0.0005	0.58	1
65	-0.0028	-3.35	0.020
70	-0.0182	-22.08	< 0.001
75-80	NA	NA	NA

Given the observed substantial decay of phage OMKO1 induced by elevated temperatures, we next sought to observe the dynamics of heat-induced decay over longer periods of time to assess whether decay would continue as exponential or appear biphasic. As expected, we found significant decay over time at 70°C (Fig 1B, ANCOVA effect of duration, $F(1, 20) = 519.1$, $p < 0.001$), and the rate of decay was similar to the prior experiment [Fig 1A slope of $\log_{10}$(percent) at 70°C = -0.0167, Fig 1B slope of $\log_{10}$(percent) of stock A = -0.0161]. We did not observe a notably biphasic decay curve. Surprisingly, biological replicates (phage stocks) had somewhat different decay dynamics, although much of this pattern was driven by a single replicate (ANCOVA effect of stock, $F(4, 20) = 2.54$, $p = 0.07$; ANCOVA interaction between stock and time, $F(4, 20) = 0.95$, $p = 0.45$).

Finally, we sought to test whether exposure to heat might affect the subsequent growth abilities of surviving phage particles. To do so, we took the phage particles that had been heat-shocked at 70°C for different durations of time and normalized their concentrations according to how many plaques they formed. Because of low titers, some populations after 270 and 360 minutes of heat shock could not be normalized, so those timepoints were excluded from analysis (see Fig S3 for data). Then, we measured how well these standardized phage suspensions suppressed the growth of host bacteria *P. aeruginosa* cultured for 12 hours (see Methods). As expected, bacterial densities initially increased, before peaking and declining as phages lysed bacterial cells (Fig S2). From these data, we extracted the peak density of bacterial population size as a proxy for gauging phage growth ability (fitness), where lower peak bacterial densities reflected higher fitness of tested phage populations. For comparison, we included two controls where bacteria were cultured in the absence of phage, in standard LB medium and in LB medium that was heat-shocked for 360 minutes.

We observed a significant effect of heat-shock exposure on the subsequent fitness of virus particles (Fig 1C), as measured by peak density of the bacterial population (ANOVA, $F(3, 15) = 14.2$, $p < 0.001$). As expected, the presence of unshocked phage OMKO1 (0 min) reduced peak bacterial density relative to the phage-free bacterial controls, indicating that the phage negatively affected bacterial growth (Table S1). Surprisingly, a history of exposure to heat shock reduced the ability of phage particles to suppress bacterial growth, permitting higher peak bacterial densities (Tukey Honest Significant Differences among all heat stress treatments showed significant differences between unshocked control of 0 minutes and

all other treatments at $p < 0.01$, see Fig 1C). However, increasing durations of heat shock exposure did not lead to further decreases in phage fitness (Tukey HSD finds no significant differences among 5 minutes through 180 minutes treatments, $p \geq 0.69$). Unexpectedly, this remained true even after extremely long heat shocks, where the survival rate was very low (e.g. after 180 minutes survival was ~0.01%; Fig. 1B). We noted that this increase in peak bacterial density could not be explained by the effect of heat-shocked medium alone, as heat shocked media had the opposite effect of reducing peak bacterial density (+ Ctrl Shock vs + Ctrl, two-sample t-test of unequal variance, $t = -4.18$, $df = 8.86$, $p = 0.002$). These results indicated that heat shock not only inactivated viral particles (Figs 1A and B), but also reduced the subsequent growth of surviving phage particles (Fig 1C).

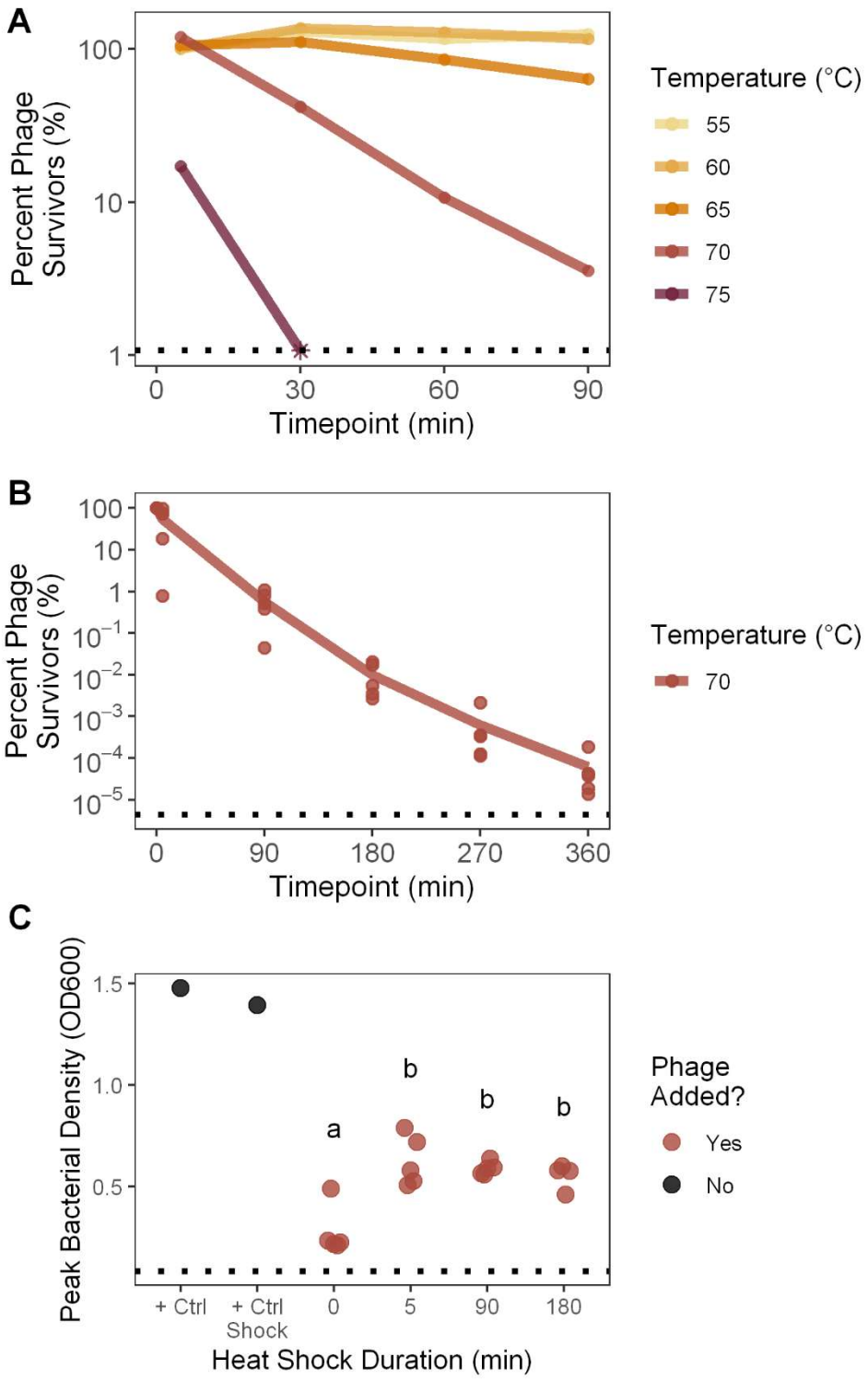

221

222 **Figure 1. Inactivation & fitness suppression of OMKO1 by thermal stress**

223 **A.** To measure phage particle survival of heat stress at different temperatures, OMKO1 was exposed to
224 one of a range of temperatures for 5, 30, 60, or 90 minutes, then titered. Percent survival is plotted

relative to the titer of the 55°C treatment after 0 minutes. The dotted line denotes the limit of detection, with the timepoint where survival fell below the limit of detection plotted as an asterisk. 80°C was also tested but caused such rapid particle decay that all measures fell below the limit of detection. **B.** To measure phage particle survival of heat stress over longer periods of time, five biological replicates of phage OMKO1 were exposed to 70°C for 5, 90, 180, 270, or 360 minutes, then titered. Percent survival is plotted relative to the source stock titer. The dotted line denotes the mean limit of detection across all five batches. **C.** To determine whether phage fitness is affected by a history of heat stress exposure, 70°C heat shocked phages or unshocked control phages (0 min) were inoculated with bacteria and grown overnight while measuring bacterial density. As a metric of phage fitness, the peak bacterial density was computationally determined. Thus, higher peak bacterial densities indicated phages with lower fitness. The dotted line denotes the absence of bacterial growth. Bacteria were also grown in the absence of phage in LB media ("+ Ctrl") or LB media that had been heat shocked for 360 mins at 70°C ("+ Ctrl Shock"). Heat shock treatments that are not significantly different from each other via Tukey Honest Significant Differences are indicated by the same shared letter (a or b).

Next, to estimate the tolerance of phage OMKO1 to saline stress, we measured phage particle survival over time in different saline concentrations, relative to starting densities. Although there was a significant effect of saline concentration on densities over time (slope of the lines in Fig 2; ANCOVA: $F(5, 23) = 5.57$, $p = 0.002$), higher saline concentrations did not accelerate phage decay (Table S2). This was likely because of the unexpected increase of phage densities in some treatments, which we ascribed to sampling variation. These findings were consistent with other data collected on a single phage stock with greater sampling density, where saline had no effect on the decay rate of phage OMKO1 (Fig S4).

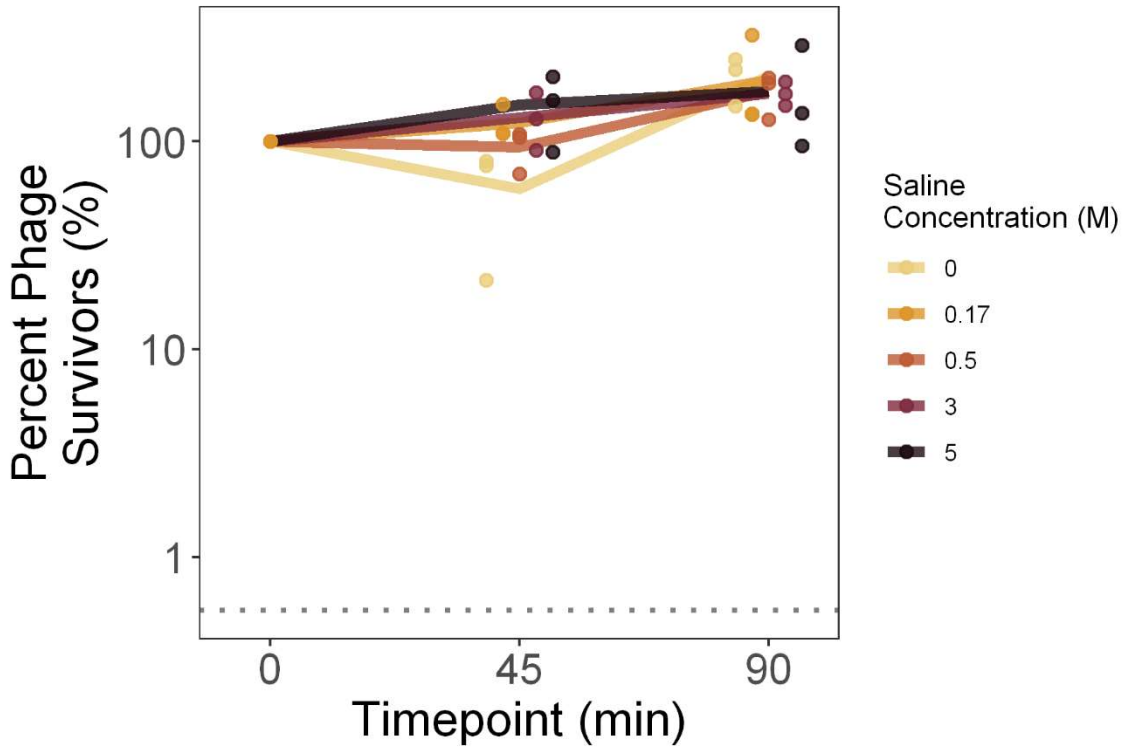

Figure 2. Phage OMKO1 decay is not accelerated by saline concentration

To measure phage particle survival of saline stress, phage OMKO1 was exposed to a range of saline concentrations then titered after 45 and 90 minutes. Percent survival is plotted relative to the titer of the LB control (0.17 M) at 0 minutes. Bold lines denote the average of the three biological replicates, with individual replicates plotted as points (horizontally offset for visualization). The mean limit of detection between the replicates is plotted as a dotted line.

To estimate the tolerance of phage OMKO1 to urea stress, we measured phage particle survival over time in different urea concentrations, relative to starting densities. Higher urea concentrations elevated the rate of decay of phage particles (Fig 3), although this trend was not significant after measures below the limit of detection were removed (slope of the lines in Fig 3; ANCOVA: $F(5, 15) = 1.19$, $p = 0.36$, Table S3). In particular, within the 90-minute assay, we observed that phage survival was unaffected by urea concentrations up to 2M, while phages decayed more rapidly in 3M and 4M. These findings were consistent with data collected on a single phage stock with greater sampling density, although there urea significantly increased decay at 1M and above (Fig S5, Table S4).

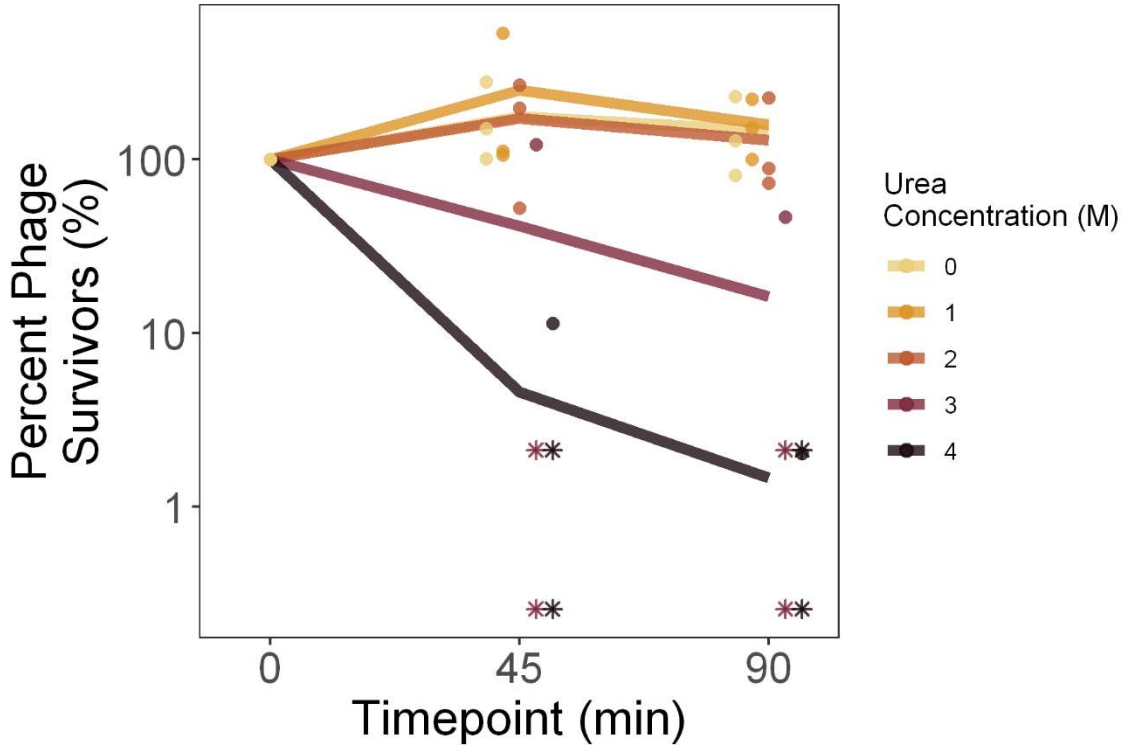

Figure 3. Degradation of phage OMKO1 under different urea concentrations.

To measure phage particle survival of urea stress, phage OMKO1 was exposed to a range of urea concentrations then titered after 45 and 90 minutes. Percent survival is plotted relative to the titer of the control (0 M) at 0 minutes. Bold lines denote the average of the three biological replicates, with individual replicates plotted as points (horizontally offset for visualization). Points which fall below the limit of detection are plotted at the limit of detection for that batch as asterisks.

Discussion

Due to increasing interest in phage therapy to complement or replace traditional chemical antibiotics, we sought to understand the stability and response of phage particles to environmental stressors. Here, we examined how the therapeutic phage OMKO1 responded to possible degradation caused by salt, urea, and heat stressors as a model of the environmental robustness of a phage therapy candidate. We observed no measurable adverse effect of salinity on phage OMKO1 survival (Fig 2), but strong effects of both increased urea concentrations (Fig 3) and elevated temperatures (Fig 1A, B) on virus survival. In addition, we found that phage particles which survived elevated temperatures had reduced fitness, as measured by their ability to suppress the growth of susceptible bacterial cells (Fig 1C).

Exposure to high temperatures both increased the decay of phage particles and decreased the fitness of particles which remained viable. Virus particles decay approximately exponentially (Fig 1B, linear on log-linear axes), with higher temperatures increasing the rate of degradation (Fig 1A), although we have limited resolution to detect a bi-phasic decay, as observed elsewhere [26]. Intriguingly, OMKO1 particles which survive exposure to heat stress experience a drastic reduction in fitness. This effect is apparent even after only five minutes of exposure, and does not become more pronounced following longer durations of heat stress (Fig 1C). Along with the observed abnormal plaque morphology after heat shock, these results indicate a strong plastic response of phage fitness to high temperature exposure. We propose three possible explanations for this observation. The first is that the population of OMKO1 particles is heterogenous in resistance to heat shock, and that stability trades off with fitness. While this sort of stability-function tradeoff is thought to be common for proteins [39, 40], this explanation is incompatible with the observation of simultaneous high survival and large decreases in fitness for two of the replicate populations (e.g. populations A and E after 5 minutes, Figs S1, S3). The second explanation is that OMKO1 particles which no longer form plaques due to heat stress may inhibit the infection of cells, possibly by competitively binding to phage receptors and blocking infection by "active" phage particles. Although this can explain improved growth of bacteria in the presence of heat-shocked phages, it cannot explain the observed changes when phages have both high survival percentages and low fitness (e.g. populations A and E after 5 minutes, Figs S1, S3). As a final explanation, we propose that high temperatures alter viral particle conformations to a lower-fitness state, an environmentally-caused damage. Thus, any exposure to heat shock alters the state and phenotype of all surviving viral particles, consistent with the observed changes in fitness following heat shock (Fig 1C). While such bistability is observed here following environmental conditions, phage particle bistability elsewhere has been previously reported to promote the evolution of novel host use [41].

We also observed that phage OMKO1 was deactivated by elevated urea concentrations, consistent with previously-published findings on other phages. For example, some of the earliest work published on this topic tested the survival of particles of coliphages (viruses that specifically infect *Escherichia coli*) over time in a 4.61M urea solution, observing decay anywhere from 0 to 7 orders of magnitude within 30 minutes [28]. Similarly, phage T4 experienced 90% decay after one minute of exposure to 2.5M urea [29]. By comparison, phage OMKO1 decayed more slowly (~95% after 45 minutes at 4M, Fig 3), suggesting that this virus had relatively greater tolerance for elevated urea concentrations compared with the limited evidence from other published studies on phage survival.

In contrast to our findings with urea, our failure to find an effect of saline stress diverged from previously-published results on other phages. Phages T2, T4, T6 and ps_1 have been reported to be deactivated when they are rapidly osmotically shocked from 4M to 0M NaCl, and several phages decay in 0M NaCl, all conditions where we observed no effect [27, 30, 31]. Experimental differences may have contributed to these divergent results, including differences in the rate of dilution and thus severity of osmotic shock, or in the relatively shorter time-lengths of our experiments. Additionally, our findings may reflect some degree of underlying differences in susceptibility to osmotic shock between different phages, where OMKO1 is more tolerant of osmotic shock and saline stress than other reported phages.

Our results are also relevant to the understanding of how environmental stressors might affect use of phage OMKO1 in human therapy. Our experiments were generally designed to exceed the range of environmental conditions that phage particles could experience during storage or within therapy applications in the human body. For example, within the human body the concentrations of salt range from roughly 30mM in urine to 135-145 mM in blood [42], all conditions where we saw no increase in phage OMKO1 decay rate (Fig 2); similarly urea concentrations range from 2.6-6.5mM in human blood up to 325mM in human urine [43], again conditions where we observed no increase in phage decay rate (Fig 3). Human body temperatures can reach a maximum of ~40°C, while phage storage conditions could reach perhaps 50°C. We found that phage OMKO1 shows no significant decay over 90 minutes at 55°C (Fig 1A), suggesting that heat stress is only relevant over these timescales at temperatures well beyond those experienced by a therapeutic phage. This, however, does not rule out the possibility of accelerated decay at lower temperatures from factors others than heat stress. These indications of the general stability of phage OMKO1 despite possible environmental stressors are promising for its further potential uses in clinical applications.

Future studies on the stability of phage OMKO1 and other therapeutic phages should expand the types of examined stressors, consider interactions between multiple stressors, and begin to more deeply elucidate the nature of the observed phage particle bistability. For instance, future work could expand on the scope of this study by considering the effects of pH and electromagnetic radiation, as well as interactions among any environmental stressors or between these stressors and storage conditions [e.g. freezing, lyophilizing (freeze drying)]. Additionally, biophysical and imaging approaches could be utilized to understand the mechanistic details behind phage particle stability and conformation, like those underlying the observed changes in phage fitness after any duration of heat stress exposure. While these experiments would deepen our understanding of phage biology and stability, our current work has revealed the limits of the stability of phage OMKO1 and highlighted intriguing nonlinear responses of phages to environmental stress, confirming the need for careful characterization and storage of therapeutic phages for widespread clinical use.

Acknowledgements

We thank Alita Burmeister, Caroline Turner, Michael Wiser, and three anonymous reviewers for helpful feedback on the manuscript, and the support for Wai Tin Lam from the Chinese University of Hong Kong.

Data Availability

All data and analysis are available at https://github.com/mikeblazanin/tin-omko1.

References

1. de Kraker ME, Davey PG, Grundmann H. Mortality and hospital stay associated with resistant Staphylococcus aureus and Escherichia coli bacteremia: estimating the burden of antibiotic resistance in

Europe. PLoS medicine. 2011;8(10):e1001104. Epub 2011/10/25. doi: 10.1371/journal.pmed.1001104. PubMed PMID: 22022233; PubMed Central PMCID: PMCPMC3191157.

2. Michael CA, Dominey-Howes D, Labbate M. The antimicrobial resistance crisis: causes, consequences, and management. Frontiers in public health. 2014;2:145. Epub 2014/10/04. doi: 10.3389/fpubh.2014.00145. PubMed PMID: 25279369; PubMed Central PMCID: PMCPMC4165128.

3. Kortright KE, Chan BK, Koff JL, Turner PE. Phage Therapy: A Renewed Approach to Combat Antibiotic-Resistant Bacteria. Cell host & microbe. 2019;25(2):219-32. Epub 2019/02/15. doi: 10.1016/j.chom.2019.01.014. PubMed PMID: 30763536.

4. Landerkin GB, Katznelson H. Stability of antibiotics in honey and sugar syrup as affected by temperature. Applied microbiology. 1957;5(3):152-4. Epub 1957/05/01. PubMed PMID: 13435725; PubMed Central PMCID: PMCPMC1057279.

5. Wick WE. Influence of antibiotic stability on the results of in vitro testing procedures. Journal of bacteriology. 1964;87(5):1162-70. Epub 1964/05/01. PubMed PMID: 5874538; PubMed Central PMCID: PMCPMC277162.

6. Samara E, Moriarty TF, Decosterd LA, Richards RG, Gautier E, Wahl P. Antibiotic stability over six weeks in aqueous solution at body temperature with and without heat treatment that mimics the curing of bone cement. Bone & joint research. 2017;6(5):296-306. Epub 2017/05/19. doi: 10.1302/2046-3758.65.bjr-2017-0276.r1. PubMed PMID: 28515059; PubMed Central PMCID: PMCPMC5457644.

7. Svahn O, Bjorklund E. Describing sorption of pharmaceuticals to lake and river sediments, and sewage sludge from UNESCO Biosphere Reserve Kristianstads Vattenrike by chromatographic asymmetry factors and recovery measurements. Journal of chromatography A. 2015;1415:73-82. Epub 2015/09/13. doi: 10.1016/j.chroma.2015.08.061. PubMed PMID: 26362805.

8. Theuretzbacher U. Global antibacterial resistance: The never-ending story. Journal of global antimicrobial resistance. 2013;1(2):63-9. Epub 2013/06/01. doi: 10.1016/j.jgar.2013.03.010. PubMed PMID: 27873580.

9. Tacconelli E, Carrara E, Savoldi A, Harbarth S, Mendelson M, Monnet DL, et al. Discovery, research, and development of new antibiotics: the WHO priority list of antibiotic-resistant bacteria and tuberculosis. The Lancet Infectious Diseases. 2018;18(3):318-27. doi: https://doi.org/10.1016/S1473-3099(17)30753-3.

10. Fazeli H, Akbari R, Moghim S, Narimani T, Arabestani MR, Ghoddousi AR. Pseudomonas aeruginosa infections in patients, hospital means, and personnel's specimens. J Res Med Sci. 2012;17(4):332-7. Epub 2012/12/26. PubMed PMID: 23267393; PubMed Central PMCID: PMCPMC3526125.

11. Mena KD, Gerba CP. Risk assessment of Pseudomonas aeruginosa in water. Reviews of environmental contamination and toxicology. 2009;201:71-115. Epub 2009/06/02. doi: 10.1007/978-1-4419-0032-6_3. PubMed PMID: 19484589.

12. Remold SK, Brown CK, Farris JE, Hundley TC, Perpich JA, Purdy ME. Differential habitat use and niche partitioning by Pseudomonas species in human homes. Microbial ecology. 2011;62(3):505-17. Epub 2011/04/20. doi: 10.1007/s00248-011-9844-5. PubMed PMID: 21503776.

13. Slekovec C, Plantin J, Cholley P, Thouverez M, Talon D, Bertrand X, et al. Tracking down antibiotic-resistant Pseudomonas aeruginosa isolates in a wastewater network. PloS one. 2012;7(12):e49300-e. doi: 10.1371/journal.pone.0049300. PubMed PMID: 23284623.

14. Garau J, Gomez L. Pseudomonas aeruginosa pneumonia. Current opinion in infectious diseases. 2003;16(2):135-43. Epub 2003/05/08. doi: 10.1097/00001432-200304000-00010. PubMed PMID: 12734446.

15. Mittal R, Aggarwal S, Sharma S, Chhibber S, Harjai K. Urinary tract infections caused by Pseudomonas aeruginosa: A minireview. Journal of Infection and Public Health. 2009;2(3):101-11. doi: https://doi.org/10.1016/j.jiph.2009.08.003.

16. Aeschlimann JR. The role of multidrug efflux pumps in the antibiotic resistance of Pseudomonas aeruginosa and other gram-negative bacteria. Insights from the Society of Infectious Diseases Pharmacists. Pharmacotherapy. 2003;23(7):916-24. Epub 2003/07/30. doi: 10.1592/phco.23.7.916.32722. PubMed PMID: 12885104.
17. Mah TF, Pitts B, Pellock B, Walker GC, Stewart PS, O'Toole GA. A genetic basis for Pseudomonas aeruginosa biofilm antibiotic resistance. Nature. 2003;426(6964):306-10. Epub 2003/11/25. doi: 10.1038/nature02122. PubMed PMID: 14628055.
18. Walters MC, 3rd, Roe F, Bugnicourt A, Franklin MJ, Stewart PS. Contributions of antibiotic penetration, oxygen limitation, and low metabolic activity to tolerance of Pseudomonas aeruginosa biofilms to ciprofloxacin and tobramycin. Antimicrobial agents and chemotherapy. 2003;47(1):317-23. Epub 2002/12/25. PubMed PMID: 12499208; PubMed Central PMCID: PMCPMC148957.
19. Seed KD. Battling Phages: How Bacteria Defend against Viral Attack. PLoS pathogens. 2015;11(6):e1004847. Epub 2015/06/13. doi: 10.1371/journal.ppat.1004847. PubMed PMID: 26066799; PubMed Central PMCID: PMCPMC4465916.
20. Chan BK, Sistrom M, Wertz JE, Kortright KE, Narayan D, Turner PE. Phage selection restores antibiotic sensitivity in MDR Pseudomonas aeruginosa. Sci Rep. 2016;6:26717. Epub 2016/05/27. doi: 10.1038/srep26717. PubMed PMID: 27225966; PubMed Central PMCID: PMCPMC4880932.
21. Gurney J, Pradier L, Griffin JS, Gougat-Barbera C, Chan BK, Turner PE, et al. Phage steering of antibiotic-resistance evolution in the bacterial pathogen, Pseudomonas aeruginosa. Evolution, Medicine, and Public Health. 2020;2020(1):148-57. doi: 10.1093/emph/eoaa026.
22. Chan BK, Turner PE, Kim S, Mojibian HR, Elefteriades JA, Narayan D. Phage treatment of an aortic graft infected with Pseudomonas aeruginosa. Evol Med Public Health. 2018;2018(1):60-6. Epub 2018/03/29. doi: 10.1093/emph/eoy005. PubMed PMID: 29588855; PubMed Central PMCID: PMCPMC5842392.
23. Pollard EC, Solosko W. The thermal inactivation of T4 and lambda bacteriophage. Biophysical journal. 1971;11(1):66-74. doi: 10.1016/S0006-3495(71)86195-7. PubMed PMID: 5539000.
24. Goldhill DH, Turner PE. The evolution of life history trade-offs in viruses. Current opinion in virology. 2014;8:79-84. Epub 2014/08/05. doi: 10.1016/j.coviro.2014.07.005. PubMed PMID: 25087040.
25. Jonczyk E, Klak M, Miedzybrodzki R, Gorski A. The influence of external factors on bacteriophages--review. Folia microbiologica. 2011;56(3):191-200. Epub 2011/06/01. doi: 10.1007/s12223-011-0039-8. PubMed PMID: 21625877; PubMed Central PMCID: PMCPMC3131515.
26. Bleichrodt JF, Blok J, Berends-Van Abkoude ER. Thermal inactivation of bacteriophage phi X174 and two of its mutants. Virology. 1968;36(3):343-55. Epub 1968/11/01. doi: 10.1016/0042-6822(68)90160-8. PubMed PMID: 5722182.
27. Anderson TF. The reactions of bacterial viruses with their host cells. The Botanical Review. 1949;15(7):464-505.
28. Burnet FM. The Classification of Dysentery-Coli Bacteriophages. III. A Correlation of the Serological Classification with Certain Biochemical Tests. Journal of Pathology and Bacteriology. 1933;37:179-84.
29. Sato GH. Activation of bacteriophage by urea. Science (New York, NY). 1956;123(3203):891-2. Epub 1956/05/18. doi: 10.1126/science.123.3203.891. PubMed PMID: 13324109.
30. Seaman PF, Day MJ. Isolation and characterization of a bacteriophage with an unusually large genome from the Great Salt Plains National Wildlife Refuge, Oklahoma, USA. FEMS microbiology ecology. 2007;60(1):1-13. Epub 2007/01/26. doi: 10.1111/j.1574-6941.2006.00277.x. PubMed PMID: 17250749.
31. Whitman PA, Marshall RT. Characterization of two psychrophilic Pseudomonas bacteriophages isolated from ground beef. Applied microbiology. 1971;22(3):463-8. Epub 1971/09/01. PubMed PMID: 4107517; PubMed Central PMCID: PMCPMC376334.

32. Dulbecco R, Vogt M. Some problems of animal virology as studied by the plaque technique. Cold Spring Harbor symposia on quantitative biology. 1953;18:273-9. Epub 1953/01/01. doi: 10.1101/sqb.1953.018.01.039. PubMed PMID: 13168995.
33. Turner PE, Draghi JA, Wilpiszeski R. High-throughput analysis of growth differences among phage strains. Journal of microbiological methods. 2012;88(1):117-21. Epub 2011/11/22. doi: 10.1016/j.mimet.2011.10.020. PubMed PMID: 22101310.
34. Singhal S, Turner PE. Effects of historical co-infection on host shift abilities of exploitative and competitive viruses. Evolution. 2021. doi: https://doi.org/10.1111/evo.14263.
35. Team RC. R: A Language and Environment for Statistical Computing [Manual]. Vienna, Austria: R Foundation for Statistical Computing; 2019. Available from: https://www.r-project.org/.
36. Wickham H, François R, Henry L, Müller K. dplyr: A Grammar of Data Manipulation [Manual]. 2019. Available from: https://cran.r-project.org/package=dplyr.
37. Wickham H. ggplot2: Elegant Graphics for Data Analysis: Springer-Verlag New York; 2016.
38. Ahlmann-Eltze C. ggsignif: Significance Brackets for 'ggplot2' [Manual]. 2019. Available from: https://cran.r-project.org/package=ggsignif.
39. Beadle BM, Shoichet BK. Structural bases of stability-function tradeoffs in enzymes. Journal of molecular biology. 2002;321(2):285-96. Epub 2002/07/30. doi: 10.1016/s0022-2836(02)00599-5. PubMed PMID: 12144785.
40. Studer RA, Christin PA, Williams MA, Orengo CA. Stability-activity tradeoffs constrain the adaptive evolution of RubisCO. Proceedings of the National Academy of Sciences of the United States of America. 2014;111(6):2223-8. Epub 2014/01/29. doi: 10.1073/pnas.1310811111. PubMed PMID: 24469821; PubMed Central PMCID: PMCPMC3926066.
41. Petrie KL, Palmer ND, Johnson DT, Medina SJ, Yan SJ, Li V, et al. Destabilizing mutations encode nongenetic variation that drives evolutionary innovation. Science (New York, NY). 2018;359(6383):1542-5. Epub 2018/03/31. doi: 10.1126/science.aar1954. PubMed PMID: 29599247.
42. Reynolds RM, Padfield PL, Seckl JR. Disorders of sodium balance. BMJ (Clinical research ed). 2006;332(7543):702-5. doi: 10.1136/bmj.332.7543.702. PubMed PMID: 16565125.
43. Liu L, Mo H, Wei S, Raftery D. Quantitative analysis of urea in human urine and serum by 1H nuclear magnetic resonance. The Analyst. 2012;137(3):595-600. Epub 12/16. doi: 10.1039/c2an15780b. PubMed PMID: 22179722.

Supplemental Material

Statistical Tables for Main Text Figures

Table S1. Phage OMKO1 suppression of peak bacterial density is robust to presence/absence of heat-shocked media in controls. Two-sample one-tailed unequal variance t-tests between both positive controls (+ Ctrl is bacteria alone, + Ctrl Shock is bacteria alone in media shocked at 70°C for 360 mins) and each of the 0 minutes heat shock populations show Bonferroni-corrected (10 tests) significant reductions in peak bacterial growth.

Contrast	Estimated Difference	df	t-value	Bonferroni-adjusted p-value
+ Ctrl – 0 mins Phage A	-1.24	5.35	-106.6	<0.001
+ Ctrl – 0 mins Phage B	-0.99	6.38	-65.2	<0.001
+ Ctrl – 0 mins Phage C	-1.26	5.77	-105.6	<0.001
+ Ctrl – 0 mins Phage D	-1.27	5.24	-109.2	<0.001
+ Ctrl – 0 mins Phage E	-1.25	6.29	-101.8	<0.001
+ Ctrl Shock – 0 mins Phage A	-1.16	5.17	-68.9	<0.001
+ Ctrl Shock – 0 mins Phage B	-0.90	6.98	-46.6	<0.001
+ Ctrl Shock – 0 mins Phage C	-1.18	5.38	-69.1	<0.001
+ Ctrl Shock – 0 mins Phage D	-1.18	5.11	-70.5	<0.001
+ Ctrl Shock – 0 mins Phage E	-1.17	5.68	-67.7	<0.001

Table S2. Multiple regression shows saline concentration does not accelerate phage decay rate. Parameter estimates of the rate of decay over time (slope) depending on saline concentration were evaluated to detect increased decay (decreased slopes) against the null hypothesis of 0 slope using one-tailed t-tests (df = 23) and a Bonferroni correction (5 tests).

Saline Concentration (M)	Estimated Coefficient	t-value	Bonferroni-adjusted p-value
0	0.013	4.41	1
LB (0.17)	0.0029	1.90	1
0.5	0.0059	1.96	1
3	0.0029	0.95	1
5	0.00090	0.30	1

Table S3. Multiple regression shows nonsignificant acceleration of OMKO1 decay by urea. Parameter estimates of the rate of decay over time (slope) depending on urea concentration were evaluated to detect increased decay (decreased slopes) against the null hypothesis of 0 slope using one-tailed t-tests (df = 15) and a Bonferroni correction (5 tests). Note that all measures below the limit of detection were excluded from analysis, limiting the power especially at 3M and 4M.

Urea Concentration (M)	Estimated Coefficient	t-value	Bonferroni-adjusted p-value
0	0.0014	0.58	1
1	-0.0020	-0.42	1
2	-0.0020	-0.42	1
3	-0.0093	-1.13	0.69
4	-0.017	-2.00	0.16

Supplemental Methods & Results

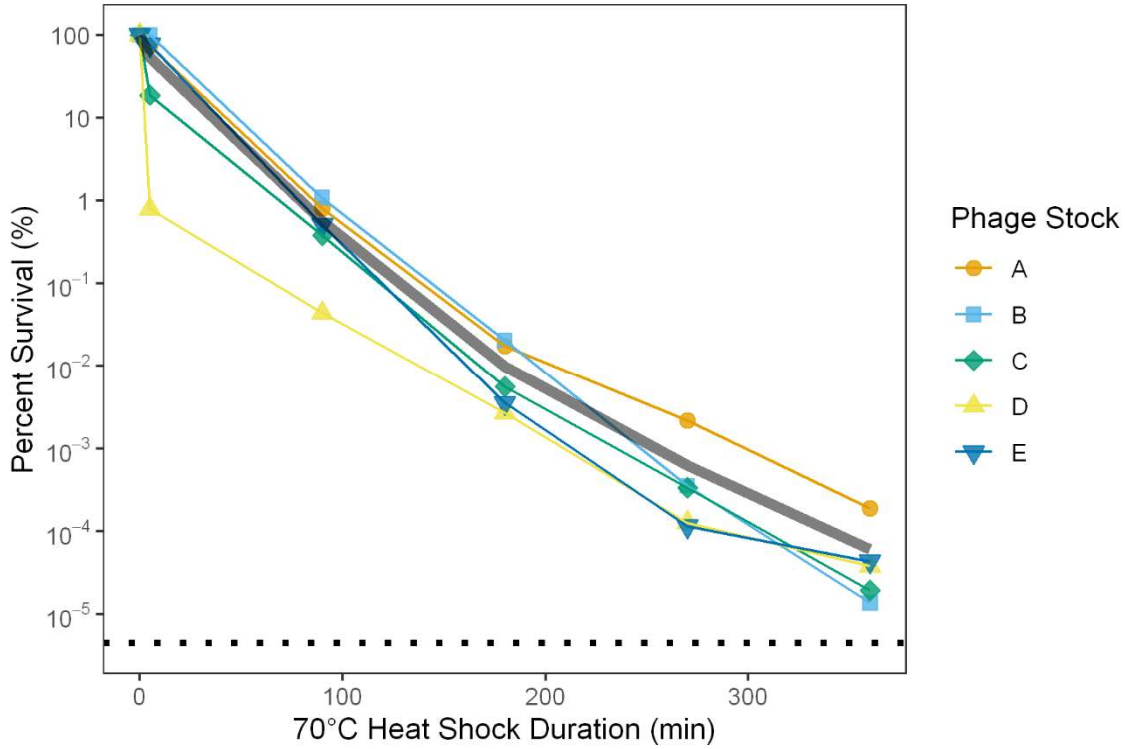

Figure S1. Inactivation of OMKO1 by 70°C thermal stress. To measure phage particle survival of heat stress over longer periods of time, five biological replicate stocks of phage OMKO1 were exposed to 70°C for 5, 90, 180, 270, or 360 minutes, then titered. Percent survival is plotted relative to the source stock titer. The dotted line denotes the mean limit of detection across all five batches. This plot shows the same data as Fig 1B, now with phage stock information shown. The gray line denotes the overall average percent survival, as plotted in Fig 1B.

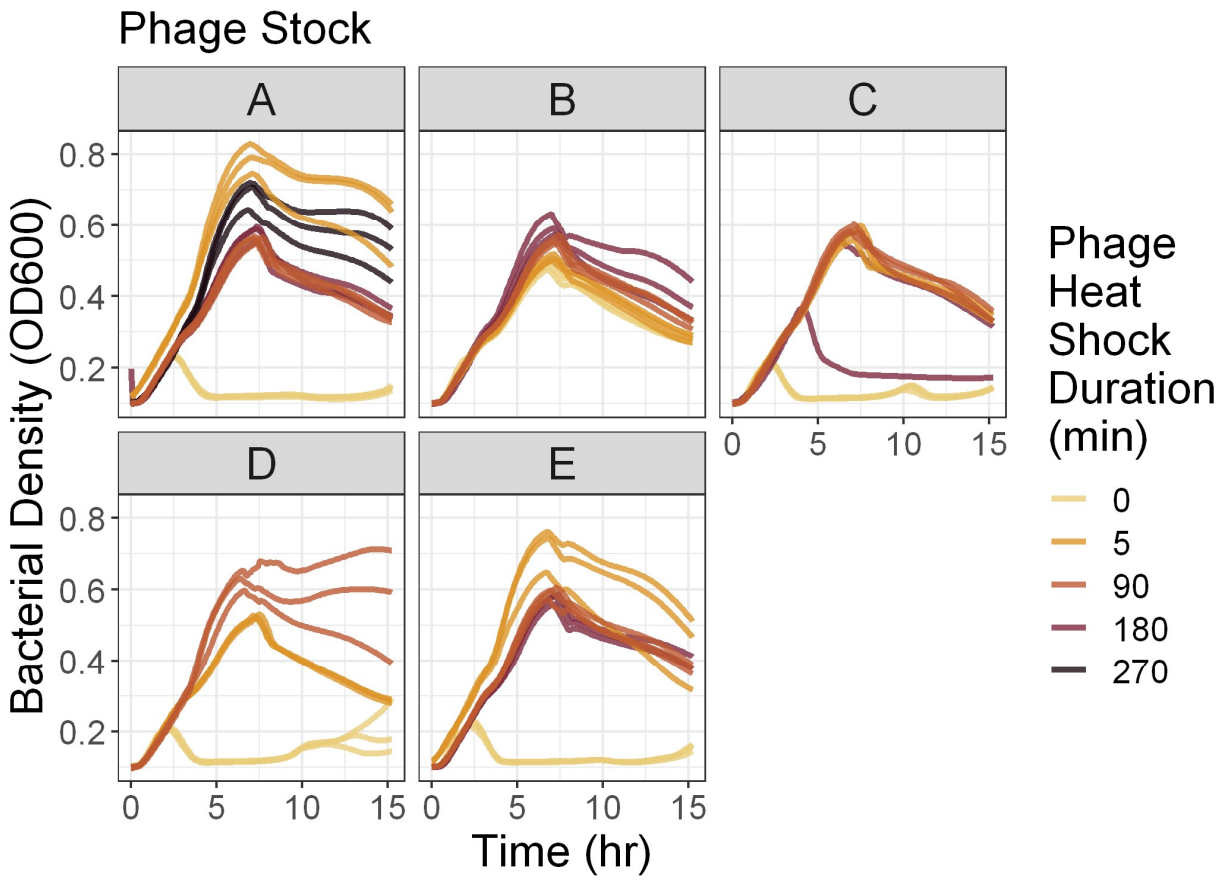

Figure S2. Bacterial growth curves in presence of post-heat shock normalized phages. Five different phage OMKO1 stocks were exposed to heat stress at 70°C for variable amounts of time, then normalized to have the same number of plaque-forming-units per volume. Bacteria and phages were inoculated into triplicate wells at constant MOI and the density of bacteria over time is plotted.

In the main text, we report the results of growth curve experiments where post-heat stress phage populations were normalized to a known concentration and grown with bacterial cells (Fig 1C). Because of low survival, at 270 and 360 minutes some stocks could not be normalized, so those timepoints were excluded from analysis and visualization. Here we present all the growth curve data, including combinations which were not inoculated with 200 pfu and 2×10^7 cfu (Fig S3).

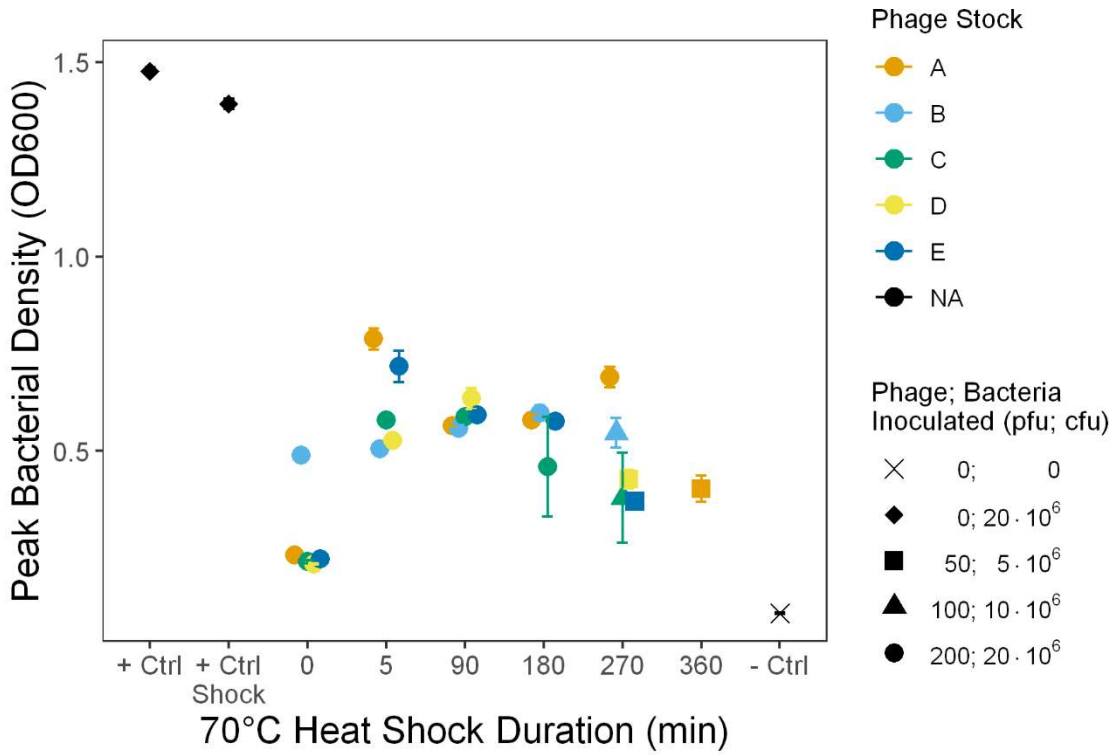

Figure S3. Fitness suppression of OMKO1 by thermal stress across all tested conditions. To determine whether phage growth was altered by exposure to heat stress among surviving phage particles, heat shocked phage particles (from Fig 1B) were inoculated with bacteria and grown overnight with repeated measurements of bacterial density. The height of the peak bacterial density was computationally determined and is plotted. Thus, this peak height is a reverse proxy for phage fitness. Error bars denote 95% confidence intervals among replicate wells. Positive control bacteria were grown in the absence of phage in LB media ("+ Ctrl") or LB media that had been heat shocked for 360 mins at 70°C ("+ Ctrl Shock"), while negative control wells contained only media. Note that, due to low survival after long durations of heat shock, some growth curves were initially inoculated with reduced numbers of bacteria and phage (holding MOI constant), confounding observed differences in peak bacterial density.

In addition to the triplicate measures of the effect of saline and urea stress on phage stability reported in the main text, we also carried out measures of their effects on a single stock with greater sampling over time and a greater range of concentrations.

To measure these effects, 10 µL of phage stock A was added to 1 mL of either urea or salt solution at a defined concentration, and vortexed to mix thoroughly. After a specified time, 50 µL were removed and immediately diluted 200-fold to terminate the stress condition. Then, the stressed samples were titered to calculate survival following stress. Controls (LB with 0.17M saline for saline stress, 0M for urea stress) were titered singly, while non-controls were titered in triplicate. We then fit a generalized linear model and carried out an ANCOVA of $\log_{10}$(percent survival) as a function of concentration (as a factor) and the

interaction between concentration and time. Values below the limit of detection and treatments that had fewer than 3 points above the limit of detection were excluded from statistical analyses and plots.

For salt stress, we exposed samples of phage OMKO1 to seven different NaCl concentrations ranging from 0M to 5M saline, including LB (0.17M saline) as a control. In each concentration treatment, subsamples were obtained at 5, 30, 60, and 90 minutes. We then measured the number of viable phage particles over time, and compared those densities to the density of phages at 5 minutes in the control to calculate percent survival. Saline concentration did not significantly alter the rate of particle decay over time (slope of the lines in Fig S4; ANCOVA: $F(8, 16) = 0.93$, $p = 0.52$).

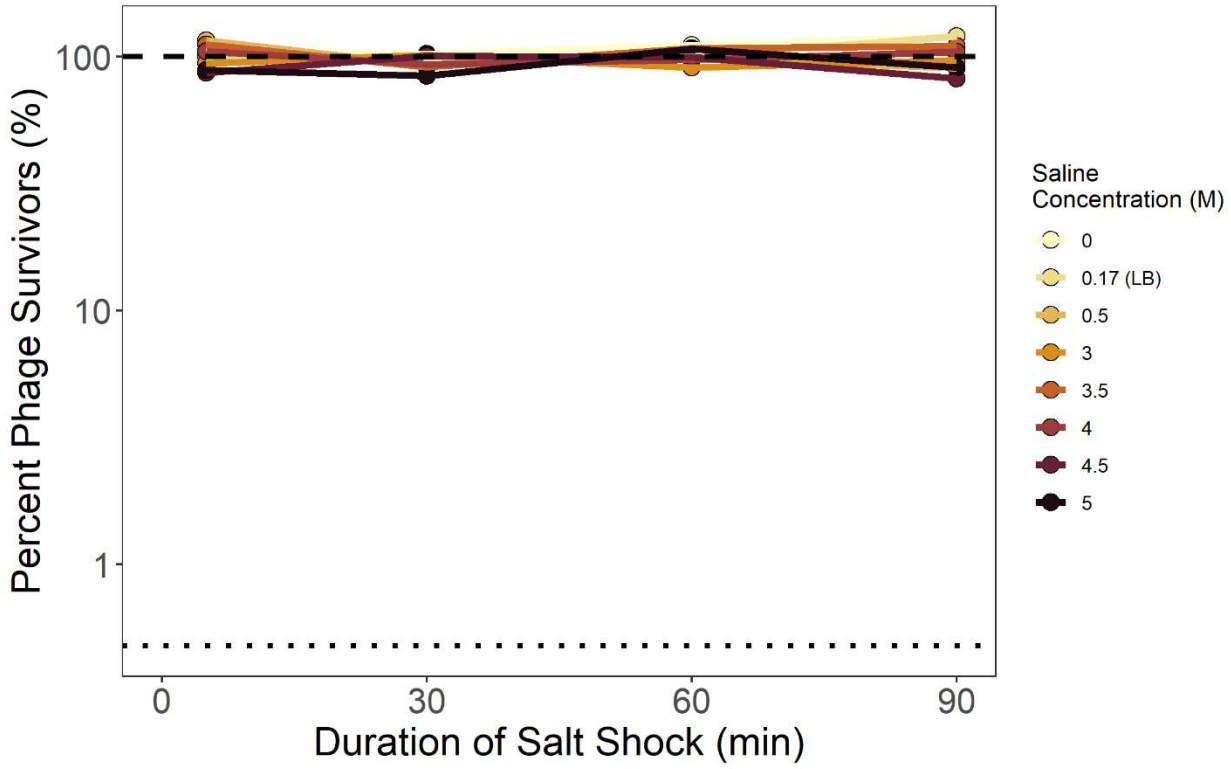

Figure S4. Phage OMKO1 stability is unaffected by saline concentration. To measure phage particle survival of saline stress, phage OMKO1 was exposed to a range of salt concentrations then titered over time. Mean percent survival was calculated and is plotted relative to the titer of the LB control (0.17M saline) at 5-minutes. The dashed line denotes 100% survival, while the dotted line denotes the limit of detection.

For urea stress, we exposed samples of phage OMKO1 to eleven different urea concentrations ranging from 0M to 10M, including 0M as a control. In each concentration treatment, subsamples were obtained at 5, 30, 60, and 90 minutes. We then measured the number of viable phage particles over time, and compared those densities to the density of phages at 5 minutes in the control to calculate percent survival. Higher urea concentrations significantly increased the rate of decay of phage particles (slope of the lines in Fig S5; ANCOVA: $F(11, 12) = 174.4$, $p < 0.001$). In particular, we observe significantly accelerated decay in all concentrations of Urea greater than 0M ($p \leq 0.01$, Table S4), with decay so rapid in concentrations of 6M and above that most measures of phage density in these treatments fell below the limit of detection.

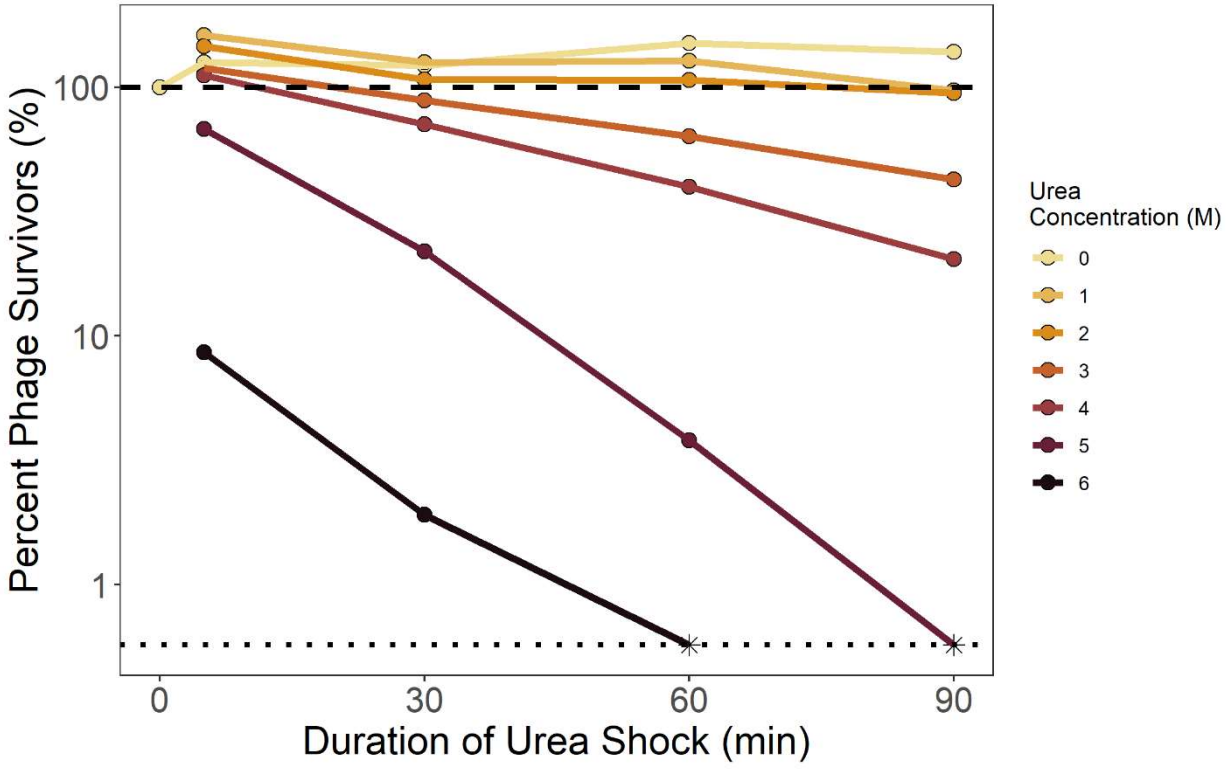

Figure S5. Urea accelerates decay of phage OMKO1. To measure phage particle survival of urea stress, phage OMKO1 was exposed to a range of urea concentrations then titered over time. Mean percent survival was calculated and is plotted relative to the titer of the control (0M) at 0 minutes. The dashed line denotes 100% survival, the dotted line denotes the limit of detection, and asterisks denote observations that fell below that limit. Concentrations 7M through 10M were tested but caused such rapid particle decay that all measures fell below the limit of detection, and are not plotted.

584 **Table S4. Multiple regression shows significant acceleration of OMKO1 decay by urea.** Parameter
585 estimates of the rate of decay over time (slope) depending on urea concentration were evaluated to
586 detect increased decay (decreased slopes) against the null hypothesis of 0 slope using one-tailed t-tests
587 (df = 12) and a Bonferroni correction (6 tests). Note that treatments with 6M through 10M urea were
588 excluded from this analysis since they did not have at least three values above the limit of detection

Urea Concentration (M)	Estimated Coefficient	t-value	Bonferroni-adjusted p-value
0	0.0014	2.56	1
1	-0.0023	-3.64	0.01
2	-0.0020	-3.08	0.002
3	-0.0052	-8.26	< 0.001
4	-0.0087	-13.7	< 0.001
5	-0.23	-22.0	< 0.001

589